

Available online at www.sciencedirect.com

ScienceDirect

journal homepage: www.elsevier.com/locate/radcr

Case Report

Preoperative localization of water clear cell giant parathyroid adenoma: A case report[☆]

Farid Gossili^{a,b,c,*}, Simona Gauduseviciene^d, Daiva Erentaite^e, Peter Iversen^f,
Charlotte E. Almasi^c

^a Department of Clinical Medicine, Aalborg University, Aalborg, Denmark

^b Department of Clinical Physiology, Viborg Regional Hospital, Viborg, Denmark

^c Department of Nuclear Medicine and Clinical Cancer Research Center, Aalborg University Hospital, Aalborg, Denmark

^d Department of Clinical Medicine, Aalborg University Hospital Thisted, Thisted, Denmark

^e Department of Pathology, Aalborg University Hospital, Aalborg, Denmark

^f Department of Nuclear Medicine and PET-Centre, Aarhus University Hospital, Aarhus, Denmark

ARTICLE INFO

Article history:

Received 23 January 2024

Revised 3 March 2024

Accepted 11 March 2024

Keywords:

[¹¹C]-Methionine PET/CT

Water clear cell

Giant parathyroid adenoma

ABSTRACT

Primary hyperparathyroidism commonly results from a solitary parathyroid adenoma. A water clear cell parathyroid adenoma represents a rare histological variant. This report presents the challenges of preoperative detection of a giant parathyroid adenoma, which was of the water clear cell variant. A case of severe hypercalcemia in a patient without clinical symptoms and equivocal findings on standard imaging modalities, in which the use of [¹¹C]-Methionine PET/CT facilitated the preoperative detection of a giant parathyroid adenoma. Histopathological examination confirmed the diagnosis of a water clear cell giant parathyroid adenoma following surgical excision. These findings highlight the significance of advanced imaging techniques in the detection and management of a rare form of parathyroid adenoma.

© 2024 The Authors. Published by Elsevier Inc. on behalf of University of Washington.

This is an open access article under the CC BY-NC-ND license

(<http://creativecommons.org/licenses/by-nc-nd/4.0/>)

Abbreviations: PHPT, primary hyper para thyroidism; PTA, para thyroid adenoma; GPA, giant parathyroid adenoma; PTH, para thyroid hormone; EANM, European Association of Nuclear Medicine; PET/CT, positron emission tomography/computed tomography; PPV, positive predictive value; SPECT, single-photon emission computed tomography; CK7, cytokeratin 7; H&E, hematoxylin and eosin; 4D-CT, four-dimensional computed tomography; MRI, magnetic resonance imaging.

[☆] Competing Interests: The authors declare that they have no known competing financial interests or personal relationships that could have appeared to influence the work reported in this paper.

* Corresponding author.

E-mail address: f.gossili@rn.dk (F. Gossili).

<https://doi.org/10.1016/j.radcr.2024.03.026>

1930-0433/© 2024 The Authors. Published by Elsevier Inc. on behalf of University of Washington. This is an open access article under the CC BY-NC-ND license (<http://creativecommons.org/licenses/by-nc-nd/4.0/>)

Background

Primary hyperparathyroidism (PHPT) stands as the third most prevalent endocrine disorder [1] and represents the leading cause for referrals of hypercalcemic patients to endocrinology outpatient clinics [2]. Solitary parathyroid adenoma (PTA) accounts for nearly 85% of PHPT cases [3,4]. Among the various types of parathyroid adenomas, the occurrence of giant parathyroid adenoma (GPA) is infrequent, characterized by adenomas weighing over 3500 mg [5]. The presence of a GPA poses clinical and surgical complexities due to elevated levels of calcium and parathyroid hormone (PTH), as well as potential mass effects [3]. Histopathological analysis frequently reveals the concurrent presence of chief cells and oxyphilic (oncocytic) cells within adenomas, a pattern that holds consistent for the predominant population of parathyroid adenomas [4]. However, rare variants include the water clear cell adenoma, distinguished by foamy to granular cytoplasm and small vacuoles with limited or absent mitochondria [6,7]. Water clear cell adenoma represents a rare etiology of PHPT [6]. The combination of a GPA with histologically confirmed water clear cell adenoma is exceptionally uncommon.

Parathyroidectomy stands as the primary treatment recommendation for young and symptomatic patients [8], employing minimally invasive techniques to reduce surgical complications and hospitalization duration. Preoperative localization of parathyroid adenoma plays a crucial role in the success of minimally invasive surgery [3]. The European Association of Nuclear Medicine (EANM) practice guidelines for parathyroid imaging advocate the use of parathyroid scintigraphy with ^{99m}Tc -Sestamibi in conjunction with cervical ultrasonography as the gold standard for preoperative localization of parathyroid adenoma. In cases where standard imaging results are negative or inconclusive, second-line imaging techniques, such as ^{11}C -Methionine positron emission tomography/computed tomography (PET/CT), are recommended [9].

The mechanism underlying the use of ^{99m}Tc -Sestamibi scintigraphy for parathyroid adenoma detection relies on the mitochondrial activity of the cells, potentially limiting its efficacy in water clear cell adenoma cases characterized by reduced or absent mitochondria [7,10]. ^{11}C -Methionine, a PET radiopharmaceutical involved in the synthesis of the PTH precursor, exhibits a high positive predictive value (PPV) of 98% for the detection of hyperfunctioning parathyroid glands [11].

In this case report, we present a patient with an exceptionally rare GPA of the water clear cell type, highlighting the challenges encountered during preoperative localization of the PTA.

Case presentation

A 57-year-old Caucasian male, with a medical history of primary hypertension and chronic mild renal dysfunction, was referred to an endocrinology outpatient clinic due to severe hypercalcemia. Laboratory analyses revealed elevated serum calcium levels of 3.11 mmol/L (reference range: 2.2–2.55 mmol/L) and albumin corrected calcium levels of 3.14 mmol/L (reference range: 2.2–2.55 mmol/L). Additionally, the patient exhibited decreased serum phosphorus levels of 0.61 mmol/L (reference range: 0.71–1.23 mmol/L) and an elevated PTH level of 19.9 pmol/L (reference range: 1.6–6 pmol/L). Consequently, given the biochemical diagnosis of primary hyperparathyroidism, the patient was expeditiously admitted for the management of hypercalcemia. Initial therapeutic measures encompassed fluid administration and infusion of bisphosphonates to establish equilibrium in the levels of serum corrected calcium. Subsequent to the implementation of these interventions, there ensued a marginal stabilization in the serum corrected calcium levels, prompting discharge of the patient. The patient was subsequently referred for further diagnostic evaluations, including ultrasound of the

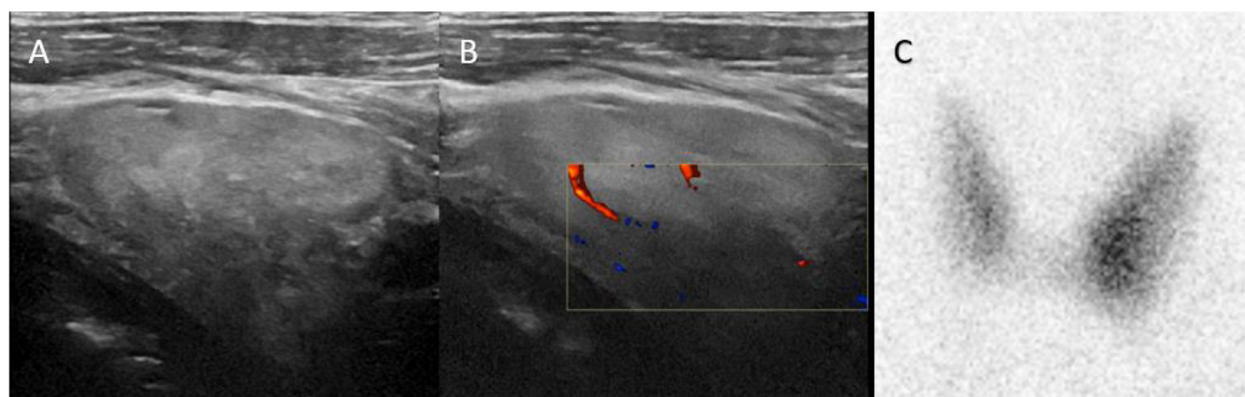


Fig. 1 – (A) Sagittal grayscale ultrasound reveals the presence of an inhomogeneous process in the caudal region of the left thyroid lobe. The sagittal dimensions of the observed abnormality were approximately 4.3 × 2.7 cm. (B) Sagittal colour Doppler images do not show any discernible pathological blood supply associated with the observed abnormality. (C) Thyroid scintigraphy presents a mildly heterogeneous uptake in the left thyroid lobe, but with no definite cold or hot areas corresponding to the nodule identified by ultrasound in the caudal region.

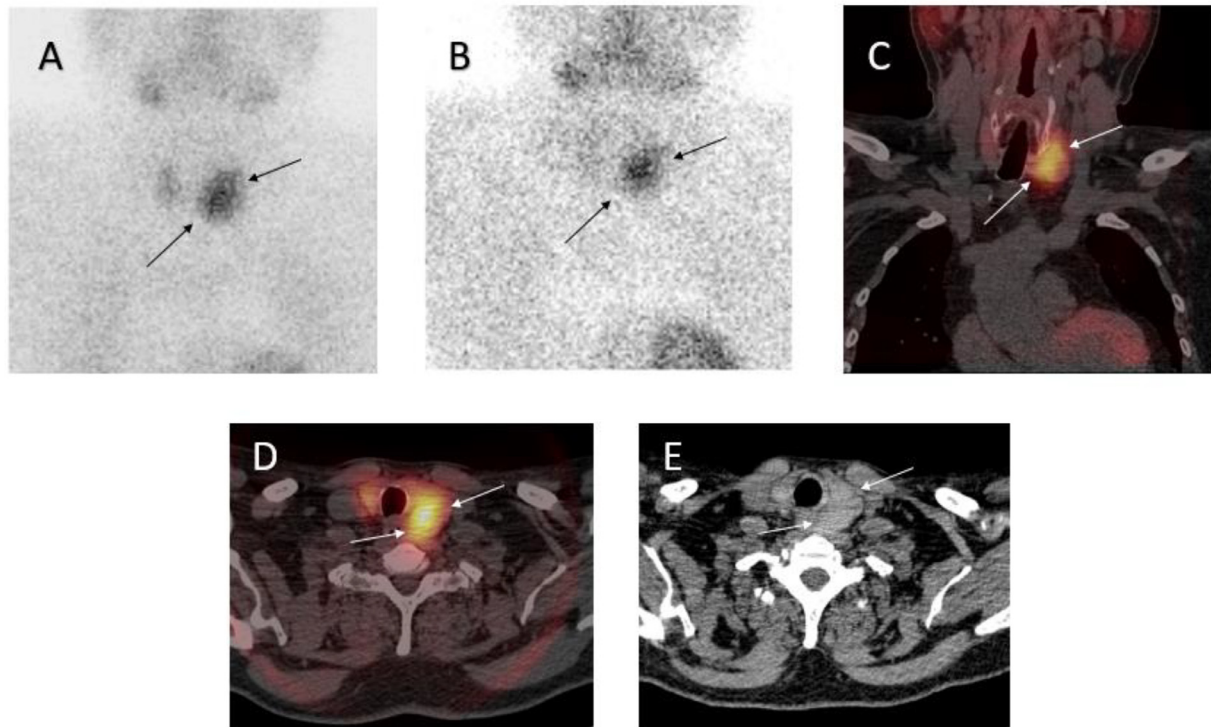


Fig. 2 – (A) Immediate ^{99m}Tc]Tc-Sestamibi SPECT show diffuse activity globally in the left thyroid lobe (arrows). (B) Delayed (2-hour) ^{99m}Tc]Tc-Sestamibi SPECT reveals persistent diffuse activity in the left thyroid lobe (arrows). (C) Delayed coronal and, (D) axial fused SPECT/CT images show persistent uptake in the posterior-caudal region of the left thyroid lobe, that could not be reliably separated from the thyroid (arrows). (E) Axial low-dose CT without contrast do not provide evidence of a parathyroid adenoma. There is no detectable difference in density between the anterior and posterior regions of the adenoma in the left thyroid lobe. These findings support the hypothesis of a thyroid adenoma rather than a parathyroid adenoma (arrows).

neck, parathyroid scintigraphy combined with supplementary thyroid scintigraphy, dual-energy X-ray absorptiometry, and CT-urography.

The ultrasound examination revealed a sizable caudal nodule measuring 4.3×2.7 cm in the left thyroid lobe, characterized by the absence of detectable internal flow as observed through colour Doppler imaging (Fig. 1). A supplementary thyroid scintigraphy was primarily carried out, which did not show either cold or warm areas correlating to the detected nodule (Fig. 1). Subsequently, dual-phase ^{99m}Tc]Tc-Sestamibi single-photon emission computed tomography (SPECT)/CT demonstrated diffuse increased uptake of sestamibi, which persisted in the late images. This uptake was localized in the posterior region of the left thyroid lobe, and could not be reliably separated from the thyroid on low-dose CT. The interpretation was that it was more likely to be consistent with nodular thyroid tissue rather than a PTA (Fig. 2). Given the equivocal findings from the standard imaging modalities, the patient was referred for ^{11}C]C-Methionine PET/CT. This advanced imaging technique revealed significant methionine uptake corresponding to a prominent lesion located posterior to the left thyroid lobe, extending in a caudal direction and

toward the esophagus, consistent with the presence of an ectopic GPA (Fig. 3). CT-urography examination showed no evidence of nephrocalcinosis, indicating the absence of calcium deposition in the renal tissue. Furthermore, dual-energy X-ray absorptiometry demonstrated mild osteopenia, as evidenced by T-scores of -0.9 and -1.0 in the lumbar spine and femoral neck, respectively.

The patient underwent subtotal parathyroidectomy on the left side, resulting in the normalization of PTH levels both intra- and postoperatively (decreasing from 32.3 to 3.3 ng/L) and during follow-up. Concurrently, calcium levels also returned to the normal range. The excised PTA had a weight of 16.8 grams. Histopathological examination revealed a nodular structure surrounded by a thin connective tissue capsule. The majority of the structure was composed of cells exhibiting abundant, clear appearing or faintly eosinophilic cytoplasm, presence of distinct cell membranes, accompanied by small hyperchromatic nuclei. These histological features were consistent with a water clear cell adenoma. Immunohistochemical analysis demonstrated positive staining for chromogranin in the mentioned cells, with focal positivity for cytokeratin 7 (CK7) (Fig. 4).

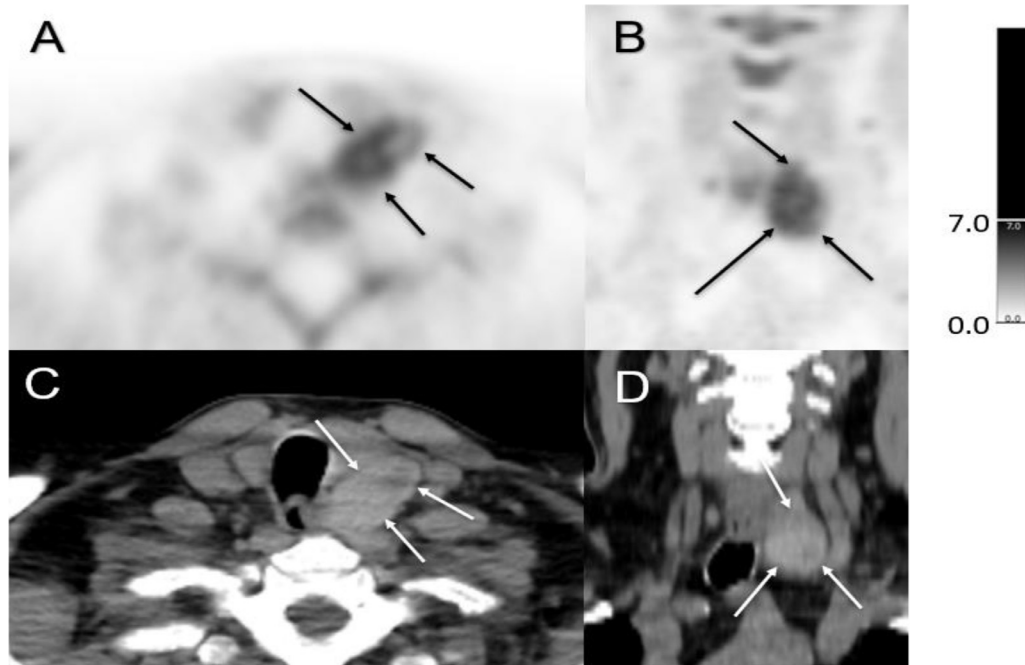


Fig. 3 – (A) Axial $[^{11}\text{C}]$ C-Methionine PET, (B) coronal $[^{11}\text{C}]$ C-Methionine PET, (C) axial noncontrast CT and (D) coronal noncontrast CT images demonstrate inhomogeneous, and in some areas, intense methionine uptake. The uptake corresponds to a larger process located posterior to the left thyroid lobe, extending caudally and toward the esophagus (position 2-5) [12]. These findings are indicative of a large, partially cystic transformed parathyroid adenoma, suggesting its probable diagnosis.

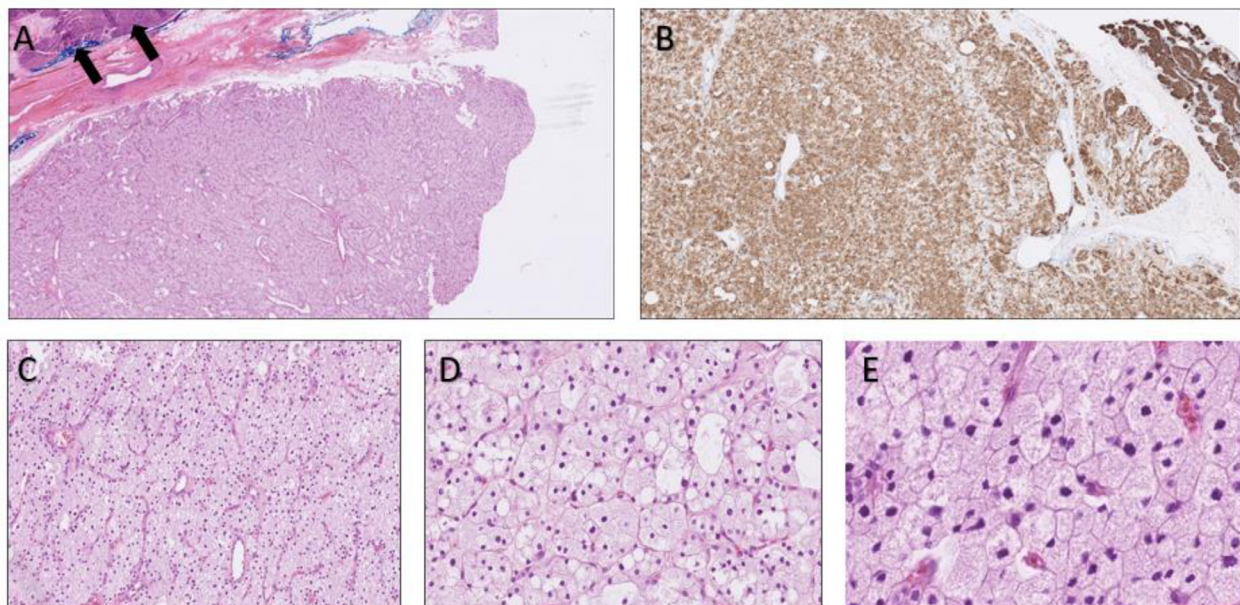


Fig. 4 – (A) Water clear cell parathyroid adenoma was identified utilizing standard hematoxylin and eosin (H&E) staining at a magnification of 12 times ($\times 12$). The adenoma exhibited encapsulation. A peripheral section of normal parathyroid tissue is evident in the upper left quadrant (indicated by black arrows). (B) The lesional cells found within the water clear cell parathyroid adenoma exhibit immunoreactivity for chromogranin A. (C) At a magnification of $\times 100$, the histological examination reveals adenoma composed of cells with clear or faint eosinophilic cytoplasm. (D) At a magnification of $\times 200$, cellular analysis demonstrates abundant clear appearing cytoplasm with finely reticulated pattern and distinct cell membranes. (E) At a magnification of $\times 400$, nuclei of the cells appear small and hyperchromatic.

Conclusions

GPA is an uncommon etiology of PHPT, and only a limited number of cases has been reported. Wong et al., in a systematic review spanning from 1952 to 2021, identified a total of 62 cases of GPA [5]. Water clear cell PTA, a distinct and rare subtype of PTA, has been documented in only a handful of cases. In a review conducted by Mohamed et al., 20 cases of water clear cell PTA were identified up until 2021 [13]. Furthermore, another study reported a total of 30 cases of water clear cell PTA in 28 patients up until the same year [7]. The combination of water clear cell and GPA represents an exceedingly rare occurrence, involving a mere 7 patients across both studies [7,13]. Documenting this rare case is crucial for clinical and research purposes, enhancing our understanding of similar patients.

Preoperative localization of water clear cell GPA presents significant challenges. The accurate localization of PTA is crucial for surgical planning, especially when considering minimally invasive approaches, as stated in the international consensus for PHPT management [9]. The recommended first-line imaging modality is [^{99m}Tc]Tc-Sestamibi scintigraphy, supplemented by ultrasound. When both modalities are concordant, the PPV for correct localization reaches 97% [14]. [^{99m}Tc]Tc-Sestamibi scintigraphy relies on the accumulation of radiotracer in cells with abundant mitochondria, exhibiting slower wash-out compared to cells with fewer mitochondria. This characteristic aids in differentiating PTAs composed of oxyphilic cells with abundant mitochondria [7,10,14]. However, water clear cell PTAs, characterized by clear cells with small or missing mitochondria [4], may result in false-negative [^{99m}Tc]Tc-Sestamibi scintigraphy findings. In a study by Juhlin et al., [^{99m}Tc]Tc-Sestamibi scintigraphy successfully visualized water clear cell PTAs in only 42% of cases [7]. In the present case, the utilization of [^{99m}Tc]Tc-Sestamibi scintigraphy failed to accurately localize the PTA, as sestamibi accumulation occurred in the left thyroid lobe in the same intensity as in the large PTA. Furthermore, the noncontrast low-dose CT did not demonstrate typical low Hounsfield unit in the adenoma [15]. Initially, the observation was inaccurately identified as indicative of nodular thyroid changes. However, the absence of SPECT/CT in the thyroid scintigraphy impeded a precise comparison between the uptake of pertechnetate and Sestamibi. Previous studies have indicated a correlation between adenoma size (regardless of histopathological subtype) and the detection rate in [^{99m}Tc]Tc-Sestamibi scintigraphy, contingent upon the hyperfunctionality of the adenoma [10,16,17]. Nevertheless, as demonstrated in the current case, the challenge of achieving accurate localization persists. Although the adenoma in this case exhibited water clear cell characteristics, its biochemical activity facilitated some detection during [^{99m}Tc]Tc-Sestamibi scintigraphy. However, due to its considerable size and the absence of discernible features indicative of a PTA on CT scan, differentiation from thyroid nodules was unfeasible, leading to an equivocal finding. Wei et al. have identified several factors contributing to a significant number of cases with equivocal imaging results in [^{99m}Tc]Tc-Sestamibi scintigraphy [18]. Importantly, in cases involving very large PTAs, in-

conclusive findings in [^{99m}Tc]Tc-Sestamibi scintigraphy can occur, even though sestamibi retention is observed in the late images, as exemplified in this particular case. According to The EANM practice guidelines for parathyroid imaging [9] in case of negative or equivocal standard imaging, second-line imaging may be performed, such as [¹⁸F]F-Fluorocholine PET/CT, [¹¹C]C-Methionine PET/CT, so-called 4-dimensional computed tomography (4D-CT), magnetic resonance imaging (MRI), [¹⁸F]F-Fluorocholine PET/4D-CT or [¹⁸F]F-Fluorocholine PET/MRI. [¹¹C]C-Methionine PET/CT was elected as second-line imaging in this case. [¹¹C]C-Methionine PET/CT detects parathyroid adenomas by exploiting their heightened uptake of radiolabeled methionine, owing to their elevated amino acid transport and metabolic activity. This selective accumulation enables precise localization with superior sensitivity compared to traditional imaging methods. The short half-life of carbon-11 facilitates swift imaging, enhancing the efficacy of [¹¹C]C-Methionine PET/CT in clinical settings. Weber et al. showed presurgical scanning with [¹¹C]C-Methionine PET/CT localized hyperfunctioning parathyroid glands in 74% of patients with negative [^{99m}Tc]Tc-Sestamibi scintigraphy [19]. The other study demonstrated the detection of 94% of pathologic parathyroid tissue using [¹¹C]C-Methionine PET/CT in a cohort of 17 patients with inconclusive preoperative localization based on [^{99m}Tc]Tc-Sestamibi scintigraphy and ultrasound [12]. According to these studies, it appears that [¹¹C]C-Methionine PET/CT holds promise as a potentially valuable modality for cases of inconclusive preoperative localization with standard imaging.

Histologically, parathyroid glands consist of a chief, oxyphil, transitional oxyphil, and water-clear cells. The clinical significance and behavior of water-clear cell PTA remain poorly understood [9]. Some studies suggest that these tumors may present with distinct clinical features, including larger tumor size compared to conventional PTAs [7]. However, further investigation is needed to determine if these differences have any prognostic implications or impact on patient outcomes. Histopathological examination remains the gold standard for the diagnosis of water-clear cell PTA. Immunohistochemical staining for parathyroid-specific markers, such as PTH, can help confirm the diagnosis and differentiate it from other clear cell neoplasms [7,13]. Owing to the scarcity of reported cases in the existing literature, the establishment of optimal management strategies for water-clear cell PTA remains unclear. Sustained surveillance is imperative to detect any recurrence or potential progression to parathyroid carcinoma, an exceedingly rare occurrence [7]. In the present case, the treatment course encompassed surgical intervention followed by a postoperative monitoring period, during which no complications arose. Subsequent to approximately 18 months of diligent follow-up, the patient's care was concluded by the endocrinology outpatient clinic, as their calcium and PTH levels normalized, and no evidence of neoplastic activity was detected.

This report not only highlights the exceptional rarity of the case under investigation and the complexities encountered in preoperative diagnosis but also elucidates the potential for [^{99m}Tc]Tc-Sestamibi scintigraphy to yield equivocal findings in the presence of a significantly large PTA, notwithstanding its hyperfunctionality. Consequently, alternative second-line

modalities, such as [¹¹C]C-Methionine PET/CT, may offer enhanced prospects for accurate preoperative localization.

Patient consent

Written informed consent was obtained from the patient for publication of this case report and accompanying images.

REFERENCES

- [1] Cetani F, Marcocci C, Torregrossa L, Pardi E. Atypical parathyroid adenomas: challenging lesions in the differential diagnosis of endocrine tumors. *Endocr Relat Cancer* 2019;26:R441–64.
- [2] Fraser WD. Hyperparathyroidism. *Lancet* 2009;374:145–58.
- [3] Walker MD, Silverberg SJ. Primary hyperparathyroidism. *Nat Rev Endocrinol* 2018;14:115–25.
- [4] Duan K, Gomez Hernandez K, Mete O. Clinicopathological correlates of hyperparathyroidism. *J Clin Pathol* 2015;68:771–87.
- [5] Wong HKG, Shipman K, Allan K, Ghabbour A, Borumandi F. Giant parathyroid tumours in primary hyperparathyroidism: a systematic review. *Langenbecks Arch Surg* 2022;407:501–16.
- [6] Yang CA, Lin JL, Dai SH, Cheng SP. Double water-clear cell parathyroid adenoma: a case report and literature review. *Endocr J* 2022;69:717–24.
- [7] Juhlin CC, Nilsson IL, Falhammar H, Zedenius J. Institutional characterisation of water clear cell parathyroid adenoma: a rare entity often unrecognised by TC-99m-sestamibi scintigraphy. *Pathology (Phila)* 2021;53:852–9.
- [8] Bilezikian JP, Bandeira L, Khan A, Cusano NE. Hyperparathyroidism. *Lancet* 2018;391:168–78.
- [9] Petranović Oščariček P, Giovanella L, Carrió Gasset I, Hindié E, Huellner MW, Luster M, et al. The EANM practice guidelines for parathyroid imaging. *Eur J Nucl Med Mol Imaging* 2021;48:2801–22.
- [10] Itani M, Middleton WD. Parathyroid imaging. *Radiol Clin North Am* 2020;58:1071–83.
- [11] Kluijfhout WP, Pasternak JD, Drake FT, Beninato T, Gosnell JE, Shen WT, et al. Use of PET tracers for parathyroid localization: a systematic review and meta-analysis. *Langenbecks Arch Surg* 2016;401:925–35.
- [12] Iversen P, Arveschoug AK, Rejnmark L, Rolighed L. C-11 methionine positron emission tomography scans improve the preoperative localization of pathologic parathyroid glands in primary hyperparathyroidism. *Scand J Surg* 2022;111:14574969211036837.
- [13] Mohamed W, El Ansari W, Al Hassan MS, Sibira RM, Abusabeib A. Water clear cell ectopic non-iatrogenic giant parathyroid adenoma in sternohyoid muscle with thyroid nodule and asymptomatic hypercalcemia due to primary hyperparathyroidism: Case report and literature review. *Int J Surg Case Rep* 2021;86:106295.
- [14] Khan AA, Hanley DA, Rizzoli R, Bollerslev J, Young JE, Rejnmark L, et al. Primary hyperparathyroidism: review and recommendations on evaluation, diagnosis, and management. A Canadian and international consensus. *Osteoporos Int* 2017;28:1–19.
- [15] Vu TH, Guha-Thakurta N, Harrell RK, Ahmed S, Kumar AJ, Johnson VE, et al. Imaging characteristics of hyperfunctioning parathyroid adenomas using multiphase multidetector computed tomography: a quantitative and qualitative approach. *J Comput Assist Tomogr* 2011;35:560–7.
- [16] Cayir D, Araz M, Yalcindag A, Cakal E. The relationship between semiquantitative parameters derived from technetium-99m methoxyisobutylisonitrile dual-phase parathyroid single-photon emission computed tomography images and disease severity in primary hyperparathyroidism. *Nucl Med Commun* 2018;39:304–11.
- [17] Kobylecka M, Koperski Ł, Chudziński W, Pihowicz P, Mączewska J, Płazińska MT, et al. Relationship between parathyroid gland scintigraphy and its histopathology, oxyphil cell content and volume: a retrospective study. *Nucl Med Rev Cent East Eur* 2019;22:29–33.
- [18] Wei WJ, Shen CT, Song HJ, Qiu ZL, Luo QY. Comparison of SPET/CT, SPET and planar imaging using 99mTc-MIBI as independent techniques to support minimally invasive parathyroidectomy in primary hyperparathyroidism: A meta-analysis. *Hell J Nucl Med* 2015;18:127–35.
- [19] Weber T, Gottstein M, Schwenger S, Beer A, Luster M. Is C-11 methionine PET/CT able to localize sestamibi-negative parathyroid adenomas? *World J Surg* 2017;41:980–5.